Earth and Planetary Science Letters 611 (2023) 118130

Contents lists available at ScienceDirect

Earth and Planetary Science Letters

journal homepage: www.elsevier.com/locate/epsl

Controls on sediment residence times in an Alpine river catchment inferred from uranium isotopes

Maude Thollon [a,b], Anthony Dosseto [a,*], Samuel Toucanne [b], Germain Bayon [b]

[a] Wollongong Isotope Geochronology Laboratory, School of Earth, Atmospheric and Life Sciences, University of Wollongong, Wollongong, NSW 2522, Australia
[b] Univ Brest, CNRS, Ifremer, Geo-Ocean, F-29280 Plouzane, France

ARTICLE INFO

Article history:
Received 9 December 2022
Received in revised form 10 March 2023
Accepted 15 March 2023
Available online xxxx
Editor: A. Jacobson

Keywords:
uranium isotopes
Var River
sediment residence time
sediment transport
hillslope

ABSTRACT

Quantifying the timescale of sedimentary processes in river basins, such as erosion, transport and deposition, and their relationships with geomorphic parameters is important in the context of ongoing climate change. In this study, we combine uranium activity ratios ($^{234}U/^{238}U$) for fine-grained (<63 μm) fluvial sediments from the Var River basin (Southern French Alps) and inferred sediment residence times, to catchment-scale spatial analysis of geomorphic parameters with the aim to investigate the factors that influence the timescale of hillslope storage and alluvial transport.

Our results show that the U isotope composition of sediments and inferred sediment residence time are mostly controlled by geomorphic parameters such as catchment elevation, slope and curvature, rather than catchment lithology. We show that sediment residence times are shorter in steep, high elevation terranes, but markedly increase wherever catchment-averaged slopes <30°, reflecting the transition from bedrock-dominated to soil-covered landscapes. Independent estimates of sediment residence times using spatial data for soil thickness and ^{10}Be-derived denudation rates show good agreement with those calculated from U isotopes. This observation validates the suitability of U isotopes to quantify sediment residence times in river catchments and for investigating how geomorphic processes control the duration of hillslope storage and fluvial transport. Furthermore, these results show that the application of U isotopes to sedimentary deposits provides robust information on the relationship between climate variability and catchment erosion, allowing us to assess the role of intrinsic vs extrinsic controls on sediment routing at the millennial timescale.

1. Introduction

Earth surface processes such as chemical weathering, sediment transport and deposition shape landscapes. Understanding the evolution of landscapes through time requires the quantification of the duration of these processes in order to assess how fast they can respond to environmental changes (see Romans et al., 2016 for a review). In this regard, the measurement of uranium-series isotopes in sediments can be particularly useful as it allows estimation of their residence time in catchment areas (DePaolo et al., 2006; Dosseto et al., 2008; Dosseto and Schaller, 2016; Granet et al., 2010). This residence time represents the time elapsed since parent material was converted into regolith, and encompasses hillslope and alluvial storage, as well as transport. In fine-grained detrital sediments, uranium (U) isotopes fractionate, with ^{234}U being preferentially lost relative to ^{238}U as a result of recoil and preferential leaching (Fleischer, 1980, 1982; Kigoshi, 1971). This time-dependent fractionation has been used to determine the *comminution age* of sediments, which represents the time elapsed since the production of sediment finer than <63 μm (DePaolo et al., 2006; Dosseto et al., 2010). In fluvial sediments, the comminution age equates to the sediment residence time; while in sedimentary deposits (continental and marine), it corresponds to the sum of both sediment residence time and depositional age. Previous studies have suggested that the sediment residence time is mostly controlled by hillslope storage and transport (Dosseto et al., 2014; Suresh et al., 2014; Yoo and Mudd, 2008). More recently, Thollon et al. (2020) showed that at a global scale, the sediment residence time is strongly dependent on the catchment size, with longer residence times occurring within large river basins displaying high sediment capacity storage. This latter study has provided first direct evidence that the U isotope composition of sediments is mostly set by the sediment residence time, hence validating the use of the ($^{234}U/^{238}U$) ratio for quantifying the timescale of sediment transport and storage in catchments. Nevertheless, a better understanding of the factors influencing the U isotope composi-

* Corresponding author.
E-mail address: tonyd@uow.edu.au (A. Dosseto).

https://doi.org/10.1016/j.epsl.2023.118130

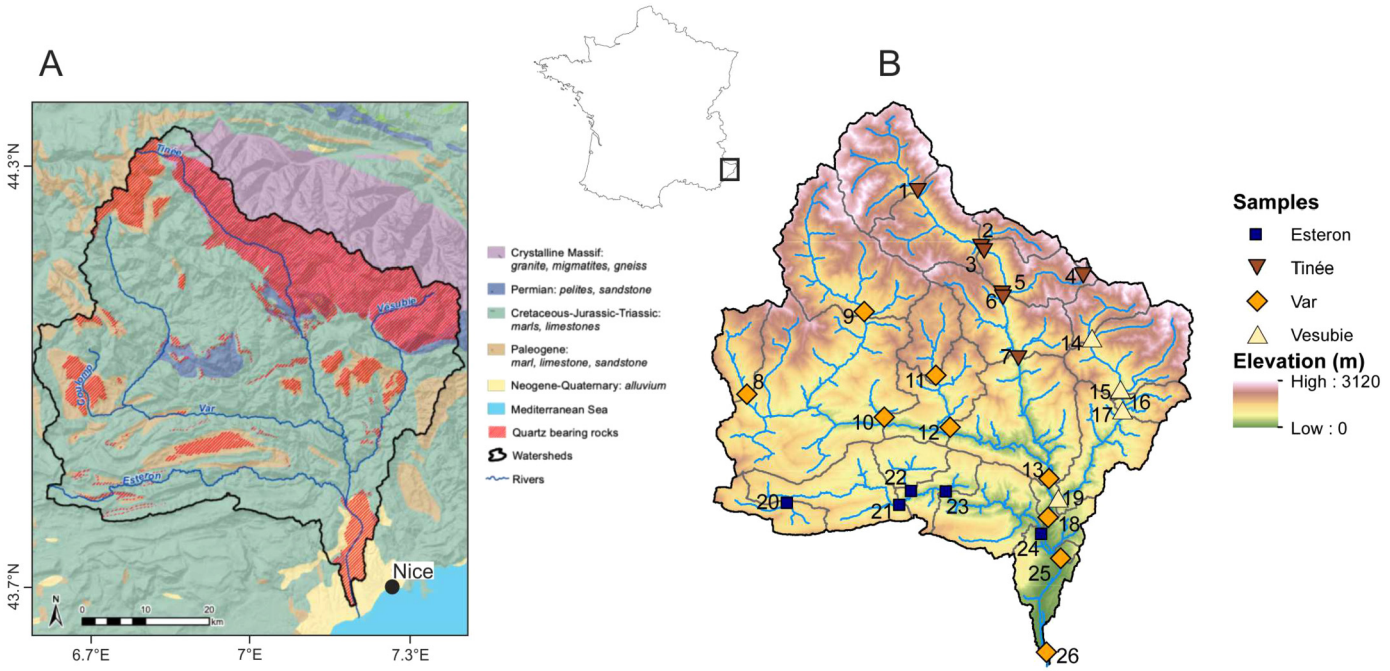

Fig. 1. (A) Simplified geological map (modified from Mariotti, 2020). (B) Digital elevation model from the Var basin derived from the French Institute National de l'Information Geographique et http://ofessionnels.ign.fr/donnees). Symbols show sample locations, labels correspond to Sample Location #'s in Table 1. Squares: Esteron River sediments, triangles: Tinée River sediments, diamonds: Var River sediments, triangles: Vésubie River sediments.

tion of fluvial sediments and inferred sediment residence times at the scale of a single catchment is required. In this study, we focused on the Var River basin, located in Southern French Alps. The mountainous part of the catchment corresponds to a reactive routing system (Allen, 2008) where short sediment residence times are expected. In contrast, the lower Var River catchment is characterised by shallower topography, thicker soils, and presumably longer sediment residence times. The diversity of geomorphic environments and lithologies encountered in the Var River basin makes it ideally well suited for investigating the various parameters controlling the U isotope composition of fluvial sediments and inferred sediment residence time. Additionally, complementary information on soil thickness and recently published ^{10}Be-derived erosion rates (Mariotti et al., 2019) across the catchment were also used to independently calculate sediment residence times.

2. Study site

The Var River catchment (2,800 km^2) is located in the Alpine mountainous region of south-eastern France (Fig. 1). The Var River is 120-km long and has four major tributaries: the Tinée, Vésubie, Esteron and Cian rivers. The Tinée and Vésubie rivers drain the high-elevation northern part of the basin, while the Esteron and Cian rivers drain the lower south-western part of the basin. Maximum elevation reaches 3,200 m in the northern part of the basin, with mean elevation of 1200 m. The average slope is 23°, with steeper slope in the north (~30° and 31° for the Tinée and Vésubie sub-catchment, respectively). The Var sediment routing system, which includes the Var turbidite system in the deep Ligurian Sea, is considered as a reactive system (Allen, 2008) because of its small alluvial plain (<50 km^2) limiting temporal on-land sediment storage (Anthony and Julian, 1999) and the close relationship observed between climates changes and sediment flux over the last glacial cycle (Bonneau et al., 2014; Jorry et al., 2011).

The northern part of the catchment is formed by the Mercantour Massif, which is mainly composed of Palaeozoic crystalline (mostly metamorphic) rocks such as gneiss, migmatites, and granitoids. The southern and the central parts of the basin are mainly composed of Mesozoic/Cenozoic carbonaceous rocks, being locally associated with various sandstones, marls and limestones (Kerckhove and Barfety, 1980; Rouire, 1979).

The Var River has an annual sediment discharge of ~ 1.63 million tons and a specific yield of 580 t/km^2/yr (Mulder et al., 1998, 1997). The sediment discharge displays significant variability over the year with moderate-to-high floods occurring both in spring, when snow melts, and in autumn/winter during intense rainfall events (Anthony and Julian, 1999; Sage, 1976) as for instance during the 2020 storm (Payrastre et al., 2022). Such high flood events can lead to stochastic erosional events associated with catastrophic discharge up to 3,700m^3/s (e.g. in November 1994), much higher than the mean annual sediment discharge of ~ 70 m^3/s (Dubar and Anthony, 1995). A Mediterranean climate dominates in the lower southern part of the basin, while mountain climate occurs in the upper river basin. The present-day vegetation in southern France is typically 'Mediterranean', being composed of grassland in high-elevation regions (>2000 m), and of temperate forest composed of drought resistant oak in lowlands (until 1,000 m) and conifers from 1,000 to 2,000 m (Beaudouin et al., 2007).

3. Methods

3.1. Spatial analysis

Catchment-averaged geomorphic parameters (elevation, slope and curvature) at each sample location were determined using a 5-m resolution digital elevation model (DEM) from the French Institute National de l'Information Geographique et Forestière (http://professionnels.ign.fr/donnees). Catchment-averaged soil thickness at each sample location was determined using the SoilGrids map with a 250 m resolution (Hengl et al., 2017). Note that the SoilGrids map is based on a compilation of soil profiles (132,193 points) and borehole drilling logs (1,574,776 points) with the addition of pseudo-observations of depth to bedrock. For geomorphic parameters and soil thickness, we computed mean, minimum and maximum values inside each sub-basin.

Table 1
Uranium concentrations, $(^{234}U/^{238}U)$ activity ratios and surface area of Var River sediments.

River	Sample Location #	Sample ID	Main lithology	Mean soil thickness (m)	Min. soil thickness (m)	Slope (°)	Elevation (m)	Curvature (m/m)	U (ppm)	2σ	$(^{234}U/^{238}U)$	2σ	S (m^2/g)	ϵ_{Nd}	2σ	U-series-derived sediment residence time (kyr)	+2σ	−2σ	Spatially-predicted soil residence time (kyr)	1σ
Esteron	20	BV-EST-05	sedimentary	15.3	8.6	18.9	1259	0.0023	2.138	0.006	0.938	0.004	13.69	−10.6	0.11	251	18	16	90	16
Esteron	21	BV-EST-04	sedimentary	16.3	8.4	22.1	1128	0.0003	1.639	0.004	0.964	0.004		−11.5	0.15	312	81	57	102	19
Esteron	22	BV-EST-02	sedimentary	20.3	12.1	20.4	815	0.0079	2.107	0.003	0.949	0.004		−10	0.13	361	105	60	120	21
Esteron	23	BV-EST-03	sedimentary	17.8	11.4	24.7	791	0.0025	1.627	0.004	0.949	0.004	11.121	−10.9	0.15	274	19	18	105	18
Esteron	24	BV-EST-01	sedimentary	18.0	10.3	22.9	926	0.0032	2.433	0.006	0.874	0.004		−11.2	0.13	643	130	84	120	24
Tinee	1	BV-TIN-05	metamorphic	18.5	2.7	29.1	2142	−0.0079	1.834	0.007	1.043	0.004	5.831	−10.6	0.1	118	5	4	69	18
Tinee	2	BV-TIN-03	metamorphic	18.6	3.7	29.4	2004	−0.0056	3.073	0.008	0.985	0.004		−11.1	0.14	251	52	36	69	18
Tinee	3	BV-TIN-04	metamorphic	17.7	5.8	31.4	2070	−0.0239	2.747	0.007	1.020	0.004		−11.1	0.11	155	29	22	66	17
Tinee	5	BV-MOL-01	metamorphic	16.3	4.3	30.8	2031	−0.0033	4.056	0.009	1.073	0.004	3.008	−10.6	0.17	66	2	1	60	16
Tinee	6	BV-TIN-02b	metamorphic	18.2	8.1	31.1	1927	−0.0073	3.080	0.006	0.999	0.004	6.99	−10.8	0.14	219	13	9	73	21
Tinee	7	BV-TIN-07	metamorphic	18.6	5.7	31.0	1859	−0.0055	2.620	0.005	0.983	0.004	6.426	−10.8	0.1	286	16	14	73	20
Var	8	BV-COU-02	sedimentary	19.1	10.5	23.4	1479	0.0012	2.272	0.006	0.869	0.004		−10.9	0.1	636	116	90	137	20
Var	9	BV-VAR-08	sedimentary	19.6	5.5	28.2	1746	−0.0044	2.434	0.007	0.947	0.004	9.86	−11	0.12	322	23	22	151	23
Var	10	BV-VAR-03	sedimentary	19.5	7.0	26.1	1473	−0.0019	2.050	0.005	0.954	0.004		−11.4	0.13	348	91	61	151	23
Var	11	BV-CIA-03	sedimentary	20.2	12.0	25.1	1634	0.0007	2.139	0.007	0.962	0.004		−10.3	0.11	300	79	48	155	24
Var	12	BV-VAR-04	sedimentary	19.9	9.8	26.6	1428	−0.0016	1.575	0.005	0.961	0.004	7.896	−11.4	0.12	346	22	22	161	26
Var	13	BV-VAR-11	sedimentary	19.2	7.0	29.3	1598	−0.0033	1.109	0.005	0.982	0.004	4.751	−10.8	0.09	393	23	17	161	27
Var	18	BV-VAR-02	sedimentary	19.1	13.8	27.6	1355	−0.0007	2.649	0.010	0.942	0.004		−11.3	0.16	381	109	64	161	27
Var	25	BV-VAR-15	sedimentary	18.9	10.0	27.1	1304	−0.0011	2.817	0.007	0.934	0.004		−10.5	0.11	411	107	69	161	28
Var	26	BV-VAR-06	sedimentary	18.9	8.3	27.5	1335	−0.0017	2.707	0.010	0.953	0.004	9.285	−10.9	0.15	306	19	18	115	14
Vesubie	14	BV-VES-03	metamorphic	18.0	4.4	30.6	2023	0.0019	2.690	0.007	1.055	0.004		−8.2	0.13	78	12	10	69	11
Vesubie	15	BV-VES-02	metamorphic	18.3	7.1	30.7	1848	−0.0015	3.472	0.011	1.026	0.004		−8	0.18	133	23	20	85	12
Vesubie	16	BV-GUA-01	metamorphic	21.1	6.2	31.2	1904	−0.0137	3.700	0.012	0.990	0.004		−9	0.11	229	48	32	96	13
Vesubie	17	BV-VES-04	metamorphic	19.1	7.6	31.3	1703	−0.0054	2.271	0.005	1.020	0.004	5.108	−8.2	0.13	189	8	7	96	14
Vesubie	19	BV-VES-01	metamorphic	18.9	8.1	31.2	1541	−0.0038	2.692	0.008	1.007	0.004		−8.4	0.17	175	33	25	96	15

Sample Location #'s refer to the numbers on Fig. 1. Sample ID's are from Bonneau et al. (2017). Soil thickness (mean and minimum), slope, elevation and curvature are catchment-averaged values at the sampling location. Details on sample collection are given in Bonneau et al. (2017).

3.2. Uranium isotopes

Twenty-six river sediment samples were collected in 2011 and 2012 along the entire Var River and its main tributaries (see details in Bonneau et al., 2017). Eleven samples were collected from the Tinée (n=6) and Vésubie (n=5) catchments, which mainly drain metamorphic granitoid rocks, and 15 samples from the Var (n=9) and Esteron (n=5) catchments, which drain sedimentary rocks (Table 1).

Samples were prepared for U isotopic analysis at the Wollongong Isotope Geochronology Laboratory (WIGL), University of Wollongong. Sediments were first wet sieved to separate the <63 µm fraction and subsequently treated to remove any biogenic, authigenic and organic components. This latter step is particularly important because these phases typically inherit a U fraction from surrounding aqueous solutions (soil water, freshwater) characterised by $(^{234}U/^{238}U) > 1$ (Andersson et al., 1998, 1992; Maher et al., 2006; Plater et al., 1988, 1992). However, great care must be taken when extracting non-detrital phases from sediments in order to prevent partial alteration of the surface of detrital gains, as ^{234}U loss occurs within the first ~30 nm of the grain's surface (Kigoshi, 1971). To this purpose, ~1 g of <63 µm sediments was treated following the sequential leaching protocol developed by Francke et al. (2018), which ensures quantitative removal of any non-detrital components without affecting detrital grains. Following leaching, a ^{229}Th-^{236}U tracer solution was added to 30 mg of the residual detrital sediment. The mixture was dissolved in HNO_3 and HF, followed by aqua regia, and finally re-dissolved in 2 mL of 7 M HNO_3 prior to U separation using ion exchange chromatography. This step was achieved using an ESI prepFAST automated chromatography system with a "THU-0500" column prefilled with AG1-X8 resin. Prior to sample loading (2 mL of 7 M HNO_3), the resin was washed with 7M HNO_3, 0.1M HCl, 6M HCl and water and then conditioned with 7M HNO_3. Following sample loading, matrix was eluted in 7M HNO_3 and uranium in 0.12M HCl. Uranium elutions were dried down and re-dissolved in 0.3M HNO_3 for isotopic analysis.

Uranium isotope analyses were performed at WIGL on a ThermoFisher Neptune Plus Multi-Collector Inductively-Coupled Plasma Mass Spectrometer (MC-ICP-MS), using an APEX HF desolvating system and a set of Jet sample and X skimmer cones. Standard bracketing was used to correct for SEM-Faraday cup yield and mass bias, using NBL U010 as primary standard (Richter and Goldberg, 2003). Analysis accuracy was determined by measuring synthetic standard NBL U005-A (Richter and Goldberg, 2003) and was consistently better than 0.5% for $(^{234}U/^{238}U)$. Total procedural blanks were measured and always <20 pg (n = 3), and their contribution is less than 0.1% to the sample $(^{234}U/^{238}U)$. Total procedural accuracy and repeatability were evaluated by replicate analyses of the reference material BCR-2 (Sims et al., 2008), showing good agreement with reference values (Table 1).

3.3. Gas sorption analysis

Specific surface area measurements were performed on 11 leached sediments by gas sorption analysis using a Quantachrome Autosorb iQ at WIGL. About ~1 g of sediments were first degassed for approximately 7.5 h with a three-steps temperature increase to 200°C (5 °C/min to 80 °C, soak time 30 min, followed by 1 °C/min to 100 °C, soak time 60 min, followed by 5 °C/min to 200 °C, soak time 300 min). Nitrogen was used as the adsorbate gas. The specific surface area was estimated using the best fit of the multi-point Brunauer–Emmett–Teller (BET) equation, with a correlation coefficient R^2 >0.999 for all measurements. The accuracy of the method was accessed by measuring the specific surface area of the certified reference material BCR-173 (Titania) (S= 8.3 m^2/g; n=2).

The obtained values for BCR-173 are within error of the certified value. The precision was estimated to be 5% (2RSD), by analysing two aliquots of the Esteron River sample EST-05.

3.4. Sediment residence time calculation

The sediment residence time was calculated as follows (DePaolo et al., 2006):

$$T_{res} = -\frac{1}{\lambda_{234}} ln\left[\frac{A_{meas} - (1 - f_\alpha)}{A_0 - (1 - f_\alpha)}\right] \quad (1)$$

where λ_{234} is the ^{234}U decay constant (in yr^{-1}), f_α the recoil loss factor, A_{meas} the measured ($^{234}U/^{238}U$) in the sediment and A_0 the ($^{234}U/^{238}U$) activity ratio at t=0. It is generally assumed that A_0 represents the U isotope ratio of the parent material, in secular equilibrium, i.e. ($^{234}U/^{238}U$) = 1, and detrital sediments should exhibit values lower than 1 as a result of preferential loss of ^{234}U. While most sediments studied here (n=18) do display ($^{234}U/^{238}U$) <1, a few (n=7) show values greater than 1, suggesting that their U isotope ratio could have evolved from a A_0 value >1. As a result, when calculating residence times, A_0 was allowed to take any values between 1 and 1.1. The upper value was taken as the maximum ($^{234}U/^{238}U$) value measured in this study.

The recoil loss factor is calculated as follows (Kigoshi, 1971; Luo et al., 2000):

$$f_\alpha = \frac{1}{4} LS\rho \quad (2)$$

where L is the ^{234}Th recoil length (taken to be 30 nm; Dosseto and Schaller, 2016), ρ the density of the sediment (assumed to be 2.65 g/cm^3) and S the surface area (m^2/g) measured by gas sorption. Because mesopores (2-50 nm in diameter) result in an overestimation of the surface area relevant to ^{234}U loss, a fractal correction needs to be applied for mesoporous materials (Bourdon et al., 2009). The shape of the adsorption-desorption isotherms during gas sorption analysis informs on the nature of the material's porosity (Sing, 1985). In this study, all isotherms were type II isotherms (Supplementary Fig. 1), characteristic of microporous or macroporous materials (Sing, 1985). Hence, no fractal correction was required and the measured surface area was directly used to calculate the recoil loss factor (Francke et al., 2018).

Sediment residence times were calculated for each sample using a Monte Carlo simulation (10,000 simulations). For each simulation, A_0 was allowed to take any random values between 1 and 1.1 (as explained above), and A_{meas} was taken randomly from the range given by the measured value ± 2SE. The surface area, S, if not measured for the sample considered, was taken randomly within the range of minimum and maximum values measured. For each sample, the resulting residence time was taken as the median of the population of simulations; and the 2SD uncertainty was calculated using the 97.9% and 2.1% quantiles of this population.

In relation to assigning values for S when it was not measured in the sample considered, we explored an alternative scenario where sediments from the Tinée and Vésubie catchments are treated separately on the one hand, and those from the Esteron and Var catchments on the other hand. In that case, S was taken randomly (for samples where it was not measured) within the range of minimum and maximum values measured in the Tinée and Vésubie sediments, when considering Tinée and Vésubie sediments; and within the range of minimum and maximum values measured in the Esteron and Var sediments, when considering Esteron and Var sediments. In this scenario, calculated residence times (Suppl. Fig. 2) are very similar to those determined using the whole range of S values from the entire dataset (Fig. 7A).

4. Results

4.1. Spatial analysis

Catchment-averaged mean elevations range from 800 (Lower Esteron; Esteron 24 in Table 1 and Fig. 1) to 2100 m (Upper Tinée; Tinée 1 in Fig. 1 and Table 1). For the Tinée sampling locations, mean elevation is between 1800 and 2100 m; between 1500 and 2000 m for the Vésubie; between 1300 and 1700 m for the Var; and between 800 and 1300 m for the Esteron. Catchment-averaged mean slopes range from 19° (Upper Esteron; Esteron 20) to 31° (Upper Tinée; Tinée3). For the Tinée sampling locations, mean slope is between 29 and 31°; between 30.6 and 31.3° for the Vésubie; between 23 and 29° for the Var; and between 19 and 25° for the Esteron. Catchment-averaged mean curvatures range from −0.024 (Upper Tinée; Tinée 3) to 0.0079 (Middle Esteron; Esteron 22). For the Tinée sampling locations, mean curvatures are all negative ranging from −0.0239 to −0.0033; they range from −0.0137 to 0.0019 for the Vésubie; from −0.0044 to 0.0012 for the Var; and they are all positive ranging from 0.0003 to 0.0079 for the Esteron. Finally, catchment-averaged mean soil thicknesses range from 1.5 (Upper Esteron; Esteron 20) to 2.1 m (Upper Vésubie; Vesubie 16). Mean soil thickness is between 1.6 and 1.9 m for the Tinée; between 1.8 and 2.1 m for the Vésubie; between 1.9 and 2.0 m for the Var; and between 1.5 and 2.0 m for the Esteron.

4.2. Uranium isotopes

Uranium concentrations for all analysed <63 µm fractions range from 1.109±0.005 (2SE internal analytical uncertainty) to 4.287±0.009 ppm (Table 1), with a mean value (2.5±0.3 ppm; 2SE, n=26) similar to that of the upper continental crust (between 2.2 and 2.8 ppm; Condie, 1993; McLennan, 2001). They display large inter-basin variability from 1.9±0.3 ppm (2SE, n=6) for the Esteron River to 3.1±0.6 ppm (2SE, n=6) for the Tinée River (Table 1). The ($^{234}U/^{238}U$) activity ratios range from 0.869±0.004 (2SE internal analytical uncertainty) to 1.073±0.004 (Table 1), with mean values of 1.02±0.02 (2SE, n=6) and 1.02±0.02 (2SE, n=5), 0.94±0.02 (2SE, n=9) and 0.93±0.03 (2SE, n=6) for the Tinée, Vésubie, Var (including Cian) and Esteron, catchments, respectively.

4.3. Specific surface area

Specific surface areas vary between 3.0±0.4 and 13.7±0.4 m^2/g (Table 1) with a mean value of 7.6±1.9 m^2/g (2SE, n=11). These are lower than most values reported in the literature. For comparison, values between 12.8 - 33.6 m^2/g were reported for 2-53 µm fractions of leached sediments from Pleistocene alluvial deposits in Australia (Handley et al., 2013); 17.2 - 18.3 m^2/g for <63 µm fractions of leached sediments from deep-sea sediments of the Var turbidite system (Francke et al., 2018) and 33.1 - 47.2 m^2/g for <63 µm fractions of leached sediments from Lake Ohrid (Francke et al., 2019). Note that sediments in Handley et al. (2013) were leached using a protocol differing from that used in this study, which follows the methodology proposed by Francke et al. (2018); Francke et al. (2019).

5. Discussion

As described above, the U isotope composition of sediments can be used to estimate their residence time in the catchment (Chabaux et al., 2008; Dosseto et al., 2008; Dosseto and Schaller, 2016; Granet et al., 2010). Nevertheless, a variety of factors can affect the U isotope composition of sediments. For instance, the lithology can presumably influence the ($^{234}U/^{238}U$) ratio of sediments as different rock types weather chemically and physically

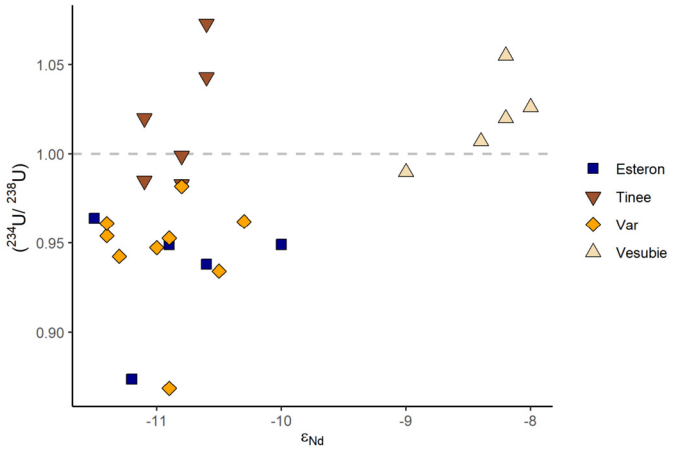

Fig. 2. ($^{234}U/^{238}U$) activity ratios as a function of Nd isotope compositions (Bonneau et al., 2017). Error bars are smaller than the symbol size if not shown. The dashed lines represent secular equilibrium for ^{234}U-^{238}U.

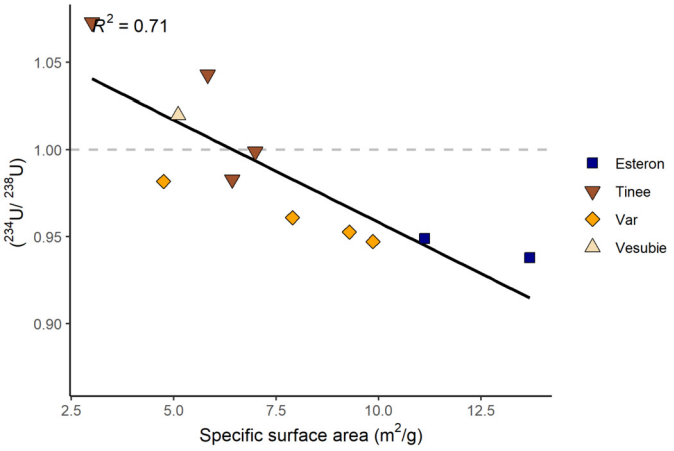

Fig. 3. ($^{234}U/^{238}U$) activity ratios as a function of specific surface area. Error bars are smaller than the symbol size if not shown. The dashed lines represent secular equilibrium for ^{234}U-^{238}U. The solid line is a linear regression through the whole dataset, shown with its R^2 value.

differently (Stallard and Edmond, 1983). Additionally, the geomorphic characteristics of the basin, which are a function of tectonics and climate, could also affect the uranium activity ratio of river sediments. Indeed, one should expect different U isotope behaviour between a basin characterised by high topography and steep slopes compared to a low-elevation basin with shallower slopes, in which sediment should be exported out more slowly (Romans et al., 2016). Below, we use our data to investigate which of these above-mentioned parameters most dominate the U isotope composition of Var river sediments.

5.1. Assessing the role of lithology on the U isotope composition of sediments

The Var River and its tributaries drain two distinct lithological units: an external alpine massif composed of igneous/metamorphic rocks in the northern part of the basin and drained by both the Tinée and the Vésubie rivers; and sedimentary deposits in the southern part of the basin, drained by the Var and the Esteron rivers. Bonneau et al. (2017) analysed neodymium isotope composition (ε_{Nd}) on the <63 µm fraction of the sediments used in this study (Table 1), showing that Vésubie sediments were characterised by ε_{Nd} values between −8 and −9, while all other sediments displayed lower ε_{Nd} values between −10 and −11.5 (Fig. 2). The Nd isotopic composition of river sediments directly reflects that of corresponding source rocks (Bayon et al., 2015; Goldstein and Jacobsen, 1987), and hence can be used as a tool to assess whether U isotope compositions may be influenced by lithology. There is no clear correlation trend between Nd and U isotope compositions (Fig. 2). Sediments with low and similar ε_{Nd} values show ($^{234}U/^{238}U$) activity ratios both lower and greater than 1. Conversely, sediments from the Tinée and Vésubie, which show very different Nd isotope compositions, both display ($^{234}U/^{238}U$) activity ratios >1. These observations suggest that lithology does not exert a major control on the U isotope composition of sediments, as previously shown in other settings (e.g. Dosseto et al., 2014; Thollon et al., 2020).

5.2. Geomorphic control on the U isotope composition of sediments

Topography exerts a major control on erosion rates (Milliman and Meade, 1983) and the weathering regime in catchments. In high-topography regions where kinetically-limited weathering conditions dominate, sediments are exported rapidly, at a rate that can be faster than the rate of silicate mineral dissolution (Stallard, 1985; West et al., 2005). Under such conditions, ^{234}U and ^{238}U isotopes show little fractionation and thus remain close to secular equilibrium with a ($^{234}U/^{238}U$) activity ratio close to 1 (Bosia et al., 2018; Dosseto et al., 2006b; Granet et al., 2010). Corresponding sediment residence times should therefore be relatively short. In contrast, in low relief regions characterised by a transport-limited weathering regime (Lupker et al., 2012; West et al., 2005), erosion rates are low and storage in weathering profiles can take place over long periods of time (>10-100's of kyr; Dequincey et al., 2002; Mathieu et al., 1995) resulting in long sediment residence times and sediments showing significant ^{234}U loss (Dosseto et al., 2006a; Suresh et al., 2014). In the study area, the Tinée and Vésubie catchments show characteristics of a kinetically-limited weathering regime, with high denudation rates (>0.25 mm/yr; Mariotti et al., 2019) and steep slopes (catchment-averaged mean slope: 29-31°). Conversely, the Var and Esteron sub-catchments show characteristics of a transport-limited weathering regime, with slower denudation rates (<0.20 mm/yr) and shallower slopes (catchment-averaged mean slope: 19-29°). Interestingly, the same dichotomy also applies to U isotopes: ($^{234}U/^{238}U$) activity ratios are >1 in the Tinée and Vésubie sediments, while ($^{234}U/^{238}U$) activity ratios are <1 in the Var and Esteron (Table 1).

Uranium isotope ratios show a negative correlation with the sediment specific surface area (Fig. 3), suggesting either that ^{234}U-^{238}U fractionation is controlled by the specific surface area of sediments or that similar process(es) control(s) the two parameters. The dependency of ^{234}U-^{238}U fractionation on the specific surface area of sediments can be evaluated by considering the sediment residence time, since its estimation combines both U isotope composition and surface area (see next section). To some extent, the ($^{234}U/^{238}U$) ratio also correlates with geomorphic parameters such as the catchment-averaged elevation, slope and curvature, while the specific surface area correlates with catchment-averaged slope and curvature (Fig. 4). These relationships illustrate the role of topography on physical weathering (and production of fine-grained sediments with high surface area), which in turn influences the U isotope composition and specific surface area of sediments: in high elevation, steep catchments, where kinetically-limited weathering dominates, the residence time of sediments may be limited, resulting in limited physical weathering and sediments with a low surface area. This shorter residence time would explain higher ($^{234}U/^{238}U$) activity ratios too, since there is less time available for ^{234}U loss. Conversely, in low relief catchments, where transport-limited weathering dominates, a reduced topography may result in longer sediment residence times, allowing for more extensive physical weathering and thus sediments with a

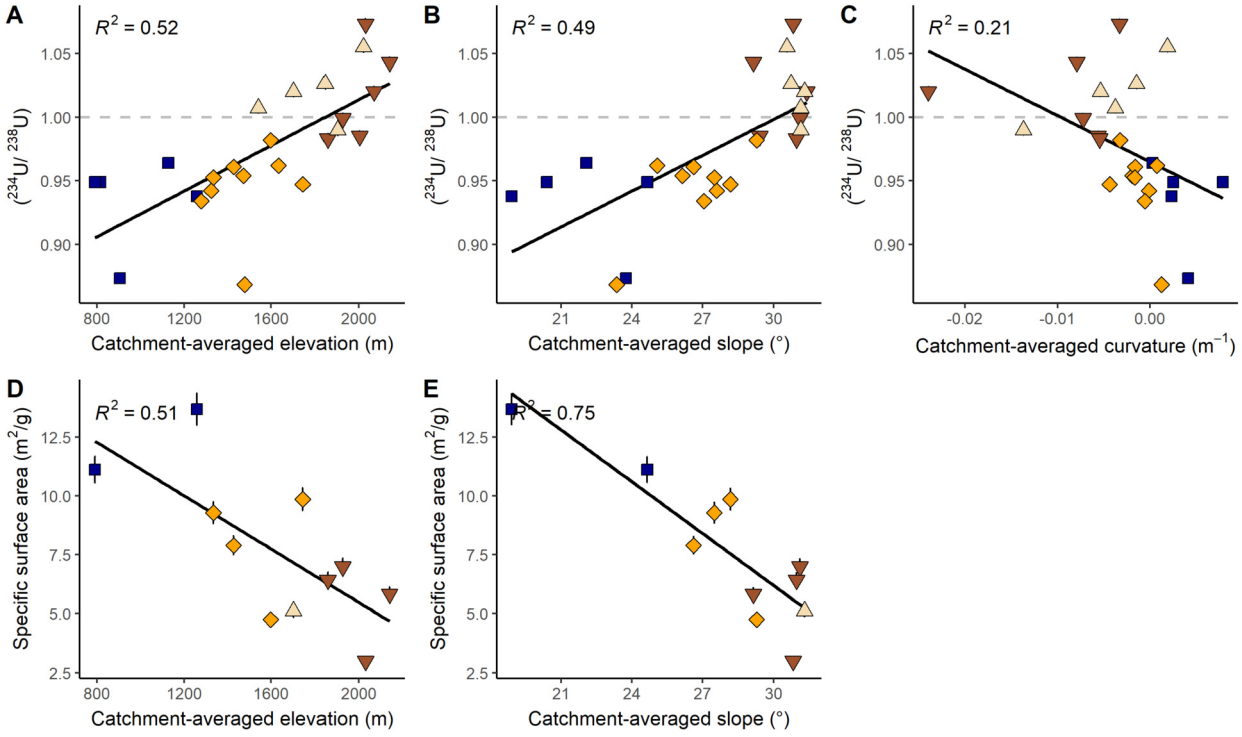

Fig. 4. ($^{234}U/^{238}U$) activity ratios as a function of catchment-averaged (A) elevation, (B) slope, and (C) curvature; and specific surface area as a function of catchment-averaged (D) elevation and (E) slope. Error bars if not shown are smaller than the symbol size. The dashed lines represent secular equilibrium for ^{234}U-^{238}U. The solid lines are linear regressions through the whole dataset, shown with their respective R^2 values. Same symbols as in Fig. 1.

higher surface area. ($^{234}U/^{238}U$) activity ratios are also lower as there is more time for ^{234}U loss.

The relationship between ($^{234}U/^{238}U$) in sediments and catchment-averaged elevation also illustrates the role of topography on the U isotope composition of fluvial sediments (Fig. 4). In high-elevation areas, soils are thin and accommodation space for alluvial storage is limited, thus associated with short sediment residence times and negligible ^{234}U loss. In contrast, in low-elevation regions, thicker soil sequences and greater accommodation space for alluvial storage are associated with longer sediment residence times and more extensive ^{234}U depletion.

5.3. Geomorphic controls on the sediment residence time

Calculated sediment residence times vary between 66 +2/-1 and 286 +16/-14 kyr for the Tinée, 78 +12/-10 and 229 +48/-32 kyr for the Vésubie, 219 +13/-9 and 636 +116/-90 kyr for the Var, and 251 +18/-16 and 643 +130/-84 kyr for the Esteron (Table 1). The highest value (643 kyr) was calculated for the lowermost sampling location of the Esteron catchment. The sediment residence time is dependent on storage in two distinct reservoirs: the hillslope and the alluvial plain. The latter is considered negligible for this catchment as the Var alluvial plain has a small extent (<2%) compared to the rest of the catchment (Julian, 1977). This is supported by the correlation between sediment residence time and catchment-averaged minimum soil thickness (Fig. 5), which suggests that the sediment residence time is mostly accounted for by storage in soils on the hillslope. Furthermore, for most catchments, the sediment residence time does not vary significantly with distance downstream (not shown) which illustrates that any alluvial storage has little incidence on the residence time. The only exception is for the Vésubie catchment, where the sediment residence time increases downstream from 78 +- 12 kyr to ~200 kyr over the first 25 km downstream from the headwater (Fig. 6). Below, the residence time remains relatively constant around 200 kyr. The increase in residence within the first 25 km could reflect an increased contribution of lower relief areas to the sediment budget. Alternatively, the residence time of ~200 kyr downstream could reflect that the sediment budget is dominated by sediments from the Gordolasque River, a tributary of the main Vésubie channel which has a sediment residence time of 230 +50/-30 kyr (sample BV-GUA-01; Table 1); however this is unlikely as this tributary is much smaller (in channel size and drainage area) than the Vésubie at the confluence.

The relationship between sediment residence time and catchment-averaged minimum soil thickness shows that a reduction of soil thickness by a factor of 2 is associated with 50% shorter residence times (Fig. 5A). Thus, this relationship shows quantitatively how sediment export efficiency varies with soil thickness. Sediment residence times also show a negative relationship with catchment-averaged elevation, and catchment-averaged slope to a lesser extent, illustrating that in steep alpine catchments, the sediment residence time is associated with thin soil cover and faster hillslope erosion (Fig. 5). These relationships are non-linear: in most catchments, residence times range between 200 and 400 kyr, except where catchment-averaged slope and elevation exceed 30° and 1500 m, respectively, in which case residence times are significantly shorter. Similarly, Heimsath et al. (2012) showed that in the San Gabriel Mountains (CA, USA) soil cover (as quantified by the Rock Exposure Index) sharply decreases for slopes greater than 30°, associated with a sharp increase in landslides and erosion rates. Here, a similar relationship between catchment-averaged minimum soil thickness and slope is observed (Fig. 5), with a possible transition from soil- to rock-dominated landscapes at a slope of 27°. In rock-dominated landscapes, an increase in slope results in a decrease in sediment residence time by a factor of ~2-5 (Fig. 5).

Sediment residence times ranging from 66 to 643 kyr are unexpectedly long, especially in Alpine catchments like the Tinée and Vésubie where soils are thin and erosion fast (for these two catch-

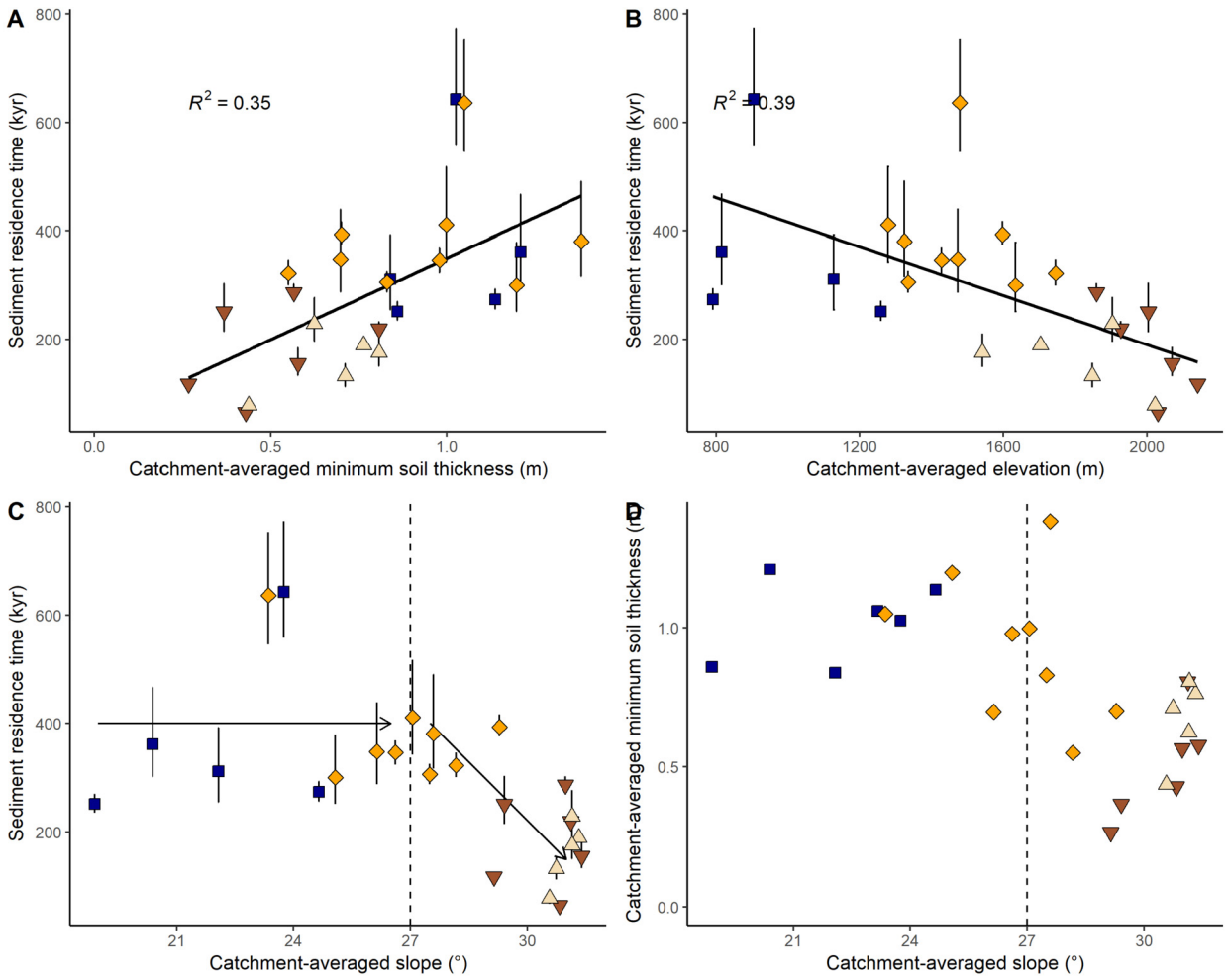

Fig. 5. Calculated sediment residence time (in kyr) as a function of catchment-averaged (A) minimum soil thickness, (B) elevation, and (C) slope; (D) catchment-averaged minimum soil thickness as a function of slope. In (C) and (D), the dashed lines show the possible transition from soil-dominated (slope <27°) to rock-dominated landscapes (slope >27°), the arrows in (C) representing how the sediment residence time shows little systematic variation where slope <27°, but decreases with increasing slope where slope >27°. Error bars if not shown are smaller than the symbol size. The solid lines are linear regressions through the whole dataset, shown with their respective R^2 values.

ments, residence times range from 66 to 286 kyr). However, Suresh et al. (2014) and Yoo et al. (2007) have shown that long residence times can be the result of slow downhill creep, even where soils are thin and erosion active. Using estimates from Yoo et al. (2007), residence times between 70 and 300 kyr can be obtained if soil is transported down hillslopes with lengths between 60 and 250 m, which are realistic values even for Alpine catchments. Thus, despite the Var River basin being a reactive sediment routing system, with little accommodation space for alluvial storage, sediment residence times generally exceed 200 kyr, reflecting long hillslope storage. When using marine sedimentary deposits of the Var River system to investigate past environmental changes (Bonneau et al., 2014, 2017; Jorry et al., 2011), such long residence times could imply that any environmental signal would be strongly dampened (Castelltort and Van Den Driessche, 2003; Jerolmack and Paola, 2010; Romans et al., 2016; Schaller and Ehlers, 2006; Simpson and Castelltort, 2012). However, the sediment residence times inferred here do not represent a sediment transport time, since they are mostly accounted for by hillslope storage, thus they do not inform on how fast environmental signals are transferred by the river to depocentres. Instead, U isotopes and the inferred sediment residence times inform on the geomorphic stores that dominate the sediment budget (Dosseto et al., 2010). They act as some sort of source tracer of geomorphic environments (e.g. fast-eroding steep relief with thin soils vs slow-eroding gentler relief with thicker soils), similarly to how Nd isotopes are a source trace of the lithology eroded. Thus, if U isotopes were to be applied to sediment deposits of the Var River system, a short residence time could be interpreted as sediments originated mostly from the Tinée and Vésubie steep catchments (and a long residence time to reflect erosion mainly in the Esteron and Var catchments).

5.4. Comparison of methods to estimate sediment residence times

Assessing the validity of sediment residence times inferred from U isotopes is difficult, as no alternative methods have been proposed to quantify the sediment residence time as it is defined (i.e. the time elapsed since onset of ^{234}U loss, associated to the onset of weathering). In-situ cosmogenic nuclides can be used to derive the residence time of sediments at the Earth's surface exposed to cosmic rays. However, in most cases, this layer is thinner that weathering profiles, thus the timescale inferred from cosmogenic nuclides would be shorter that the sediment residence time defined to encompass storage in weathering profiles, colluvial and alluvial transport (Dosseto and Schaller, 2016). Here, we calculated an independent estimate of the sediment residence by combining spatial data for estimated soil thickness (SoilGrids, Hengl et al., 2017; Shangguan et al., 2017) and catchment-averaged denudation rates derived from in-situ ^{10}Be (Mariotti et al., 2019). For each location where sediments were sampled for in-situ ^{10}Be, soil thickness and denudation rates were spatially averaged by the area

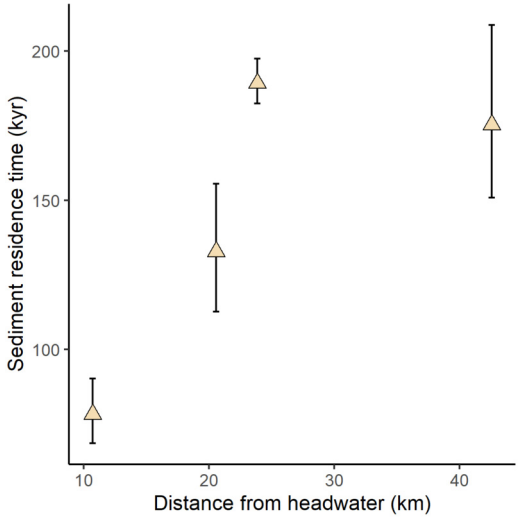

Fig. 6. Calculated sediment residence time (in kyr) as a function of the distance from the headwater (in km) for the Vésubie catchment. Errors bars are 2SE.

drained at the sample location. Thus, the ratio of soil thickness to denudation rate yields a spatially averaged soil residence time (Table 1). Because there is little accommodation space for alluvial storage, this soil residence time can be considered equivalent to the sediment residence time and compared to the sediment residence time inferred from U isotopes at the same location.

Sediment residence times inferred from U isotopes show a positive relationship with soil residence times inferred from the combination of soil thickness and ^{10}Be-derived denudation rates (R^2= 0.45, Fig. 7). The latter are systematically lower (by an average factor of ~2.5) than the former. This discrepancy could be explained if 1) denudation rates are over-estimated, 2) catchment-average soil thickness is under-estimated, or 3) the residence time derived from U isotopes is over-estimated. In the first case, Yanites et al. (2009) has shown than in-situ ^{10}Be can over-estimate denudation rates in catchments where landslides are prominent, in particular where drainage area is <100 km^2, as it is the case here especially for the Tinée and Vésubie catchments. Furthermore, in catchments that experienced glaciations and where soils were stripped ~20,000 yr ago (as it is the case here), denudation rates derived from in-situ ^{10}Be in sediments can be overestimated by a factor of 2 (Ackerer et al., 2016, 2022). In the second case, catchment-averaged soil thickness is the 'Depth to bedrock' derived from machine learning modelling using a global database of soil profiles (Hengl et al., 2017; Shangguan et al., 2017). Soil thicknesses used in our calculations range from 15 to 21 m, which is greater than what is expected at least in alpine catchments. Thus it is unlikely that soil thickness is under-estimated yielding residence times that are too short. In the third case, it is possible that the measured (^{234}U/^{238}U) activity ratios and/or surface area are too low. Lowering U isotope ratios during sample preparation is unlikely as whether authigenic phase removal was incomplete or grain leaching was too aggressive, this would result in ratios that are too high (Francke et al., 2018). As indicated above, surface area values determined here are lower than those reported in the literature, by a factor of up to 10. While it is unclear why <63 µm fractions have such low surface area in the Var catchment, surface area correlates with the U isotope ratio (Fig. 3) and geomorphic parameters such as catchment elevation or slope (Fig. 4). Thus, any under-estimation of the surface area is likely to be systematic. When only including catchments where the surface area was measured, while the offset between the two residence times still exist, data display a better correlation (R^2 = 0.69; Fig. 6B). This illustrates that assuming values for the surface area in catchments where it was not measured may not be appropriate in some cases, and suggest that residence times >600 kyr calculated here are erroneous. Another possibility is to consider that ^{234}U has not been lost by direct recoil only (as Equation (1) assumes). Preferential leaching alone cannot account for this additional loss, as all the ^{234}U available for preferential leaching is removed after 200 yr (Dosseto and Schaller, 2016). Alternatively, ^{234}U could be leached from newly exposed tracks as a consequence of mineral dissolution during hillslope storage and alluvial transport (Cogez et al., 2018; Dosseto and Schaller, 2016). Using Equation (12) in Dosseto and Schaller (2016), to solve the discrepancy between U-series and spatial data/^{10}Be residence times, it would require the fraction of ^{234}U released from newly exposed recoil tracks during mineral dissolution to be ~0.25 (i.e. a 1/4 of the ^{234}U lost is leached from new tracks exposed during dissolution). While this hypothesis cannot be tested with our current dataset, future work should aim at further investigating the factors explaining the observed discrepancy between U isotopes- vs ^{10}Be-derived residence times. Regardless the source of the discrepancy in absolute values between residence times calculated by two different methods, their correlation indicates that U isotopes in sediments are able to identify the range and variability of sediment residence times, and spatial data on soil thickness combined to in-situ ^{10}Be measurements are a suitable alternative method.

6. Conclusion and perspectives

In this study, we investigated the different factors that can influence the U isotope composition of fluvial sediments. We found that catchment lithology does not play a significant role; instead, geomorphic parameters such as catchment elevation, slope and curvature, are the dominant factors. In high relief regions, (^{234}U/^{238}U) is close to 1 or greater than 1, because short storage in thin soils and fast sediment export limits ^{234}U loss. Conversely, (^{234}U/^{238}U) is low in low relief regions illustrating the increased hillslope storage in thicker soil sequences resulting in more extensive ^{234}U loss. The sediment residence time inferred from U isotopes also correlate with geomorphic parameters, confirming expectations that the residence time is shorter in steep, high elevation terranes, and providing some validation of the method. Sediment residence times sharply decrease where catchment-averaged slopes exceed 30°, reflecting the transition from soil-covered to bedrock-dominated landscapes.

The sediment residence time was also estimated independently using spatial data of soil thickness and ^{10}Be-derived denudation rates and shows good agreement with that calculated using U isotopes. This test further demonstrates the suitability of using U isotopes to infer sediment residence times. Our results show that despite the Var River basin being a reactive sediment routing system, with little accommodation space for alluvial storage, sediment residence times generally exceed 200 kyr, reflecting long hillslope storage. Uranium isotopes and inferred sediment residence times act as a tracer of geomorphic environments (e.g. steep terranes with thin soils vs gentler relief with thicker soils). Their application to marine sediment deposits of the Var River system could shed a light on how its sediment budget responds to climate variability at the millennial scale (e.g. change in sediment origin between the steep Tinée and Vésubie catchments vs the lower relief catchments of the Esteron and Var Rivers). One limitation of this approach is the possible overestimation of sediment residence times. However, despite this limitation, calculated sediment residence times show clear relationships with geomorphic parameters and alternative methods of estimating residence time; and in sediment records, it has been shown that U isotopes and inferred residence times correlate strongly with Quaternary climatic and vegetation changes

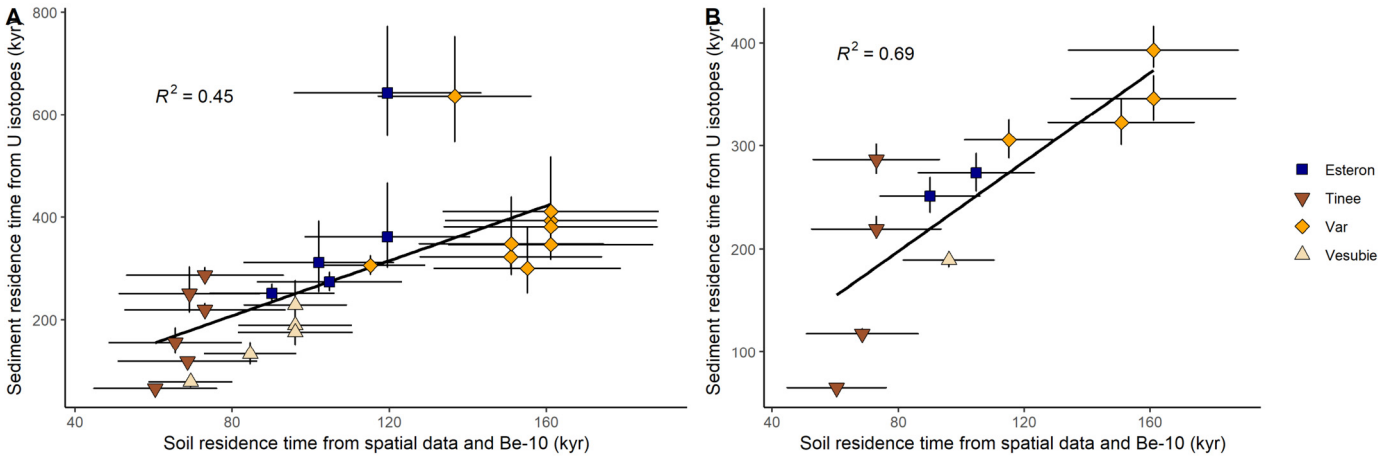

Fig. 7. Sediment residence times calculated using U isotopes as a function of soil residence times estimated using catchment-averaged soil thickness (SoilGrids) and the ^{10}Be-derived denudation rate at each sampling location (Mariotti et al., 2019). A: all catchments; B: only catchments where the surface area was measured. The solid line is a linear regression through the whole dataset, shown with its R^2 value. Error bars are at the 1σ level for the soil residence time (propagated from uncertainties on denudation rates) and at the 2σ level for the sediment residence time.

(Dosseto et al., 2010; Dosseto and Schaller, 2016; Francke et al., 2019; Rothacker et al., 2018).

CRediT authorship contribution statement

AD and SM designed the study, MT conducted the analytical work, MT, AD, SM and GB interpreted the data and wrote the manuscript.

Declaration of competing interest

The authors declare that they have no known competing financial interests or personal relationships that could have appeared to influence the work reported in this paper.

Data availability

Data will be made available on request.

Acknowledgements

MT was supported by a joint IFREMER - University of Wollongong postgraduate scholarship. This work was supported by ISblue project, Interdisciplinary graduate school for the blue planet (ANR-17-EURE-0015) and co-funded by a grant from the French government under the program "Investissements d'Avenir". We thank Korin Brown and Alexandru Codilean for help with GIS analysis, and Alexander Francke for help in the laboratory. ST is grateful to L. Bonneau, S.J. Jorry and R. Silva Jacinto (Ifremer) for assistance during fieldwork.

Appendix A. Supplementary material

Supplementary material related to this article can be found online at https://doi.org/10.1016/j.epsl.2023.118130.

References

Ackerer, J., Chabaux, F., Van der Woerd, J., Viville, D., Pelt, E., Kali, E., Lerouge, C., Ackerer, P., di Chiara Roupert, R., Négrel, P., 2016. Regolith evolution on the millennial timescale from combined U–Th–Ra isotopes and in situ cosmogenic 10Be analysis in a weathering profile (Strengbach catchment, France). Earth Planet. Sci. Lett. 453, 33–43.

Ackerer, J., Van der Woerd, J., Mériaux, A.S., Ranchoux, C., Schäfer, G., Delay, F., Chabaux, F., 2022. Quantifying geomorphological evolution from 10Be denudation rates: Insights from high-resolution depth profiles, topsoils, and stream sediments (Strengbach CZO, France). Earth Surf. Process. Landf. 47, 3239–3258.

Allen, P.A., 2008. Time Scales of Tectonic Landscapes and Their Sediment Routing Systems.

Andersson, P.S., Porcelli, D., Wasserburg, G.J., Ingri, J., 1998. Particle transport of ^{234}U-^{238}U in the Kalix River and the Baltic Sea. Geochim. Cosmochim. Acta 62, 385–392.

Andersson, P.S., Wasserburg, G.J., Ingri, J., 1992. The sources and transport of Sr and Nd isotopes in the Baltic Sea. Earth Planet. Sci. Lett. 113, 459–472.

Anthony, E.J., Julian, M., 1999. Source-to-sink sediment transfers, environmental engineering and hazard mitigation in the steep Var River catchment, French Riviera, southeastern France. Geomorphology 31, 337–354.

Bayon, G., Toucanne, S., Skonieczny, C., André, L., Bermell, S., Cheron, S., Dennielou, B., Etoubleau, J., Freslon, N., Gauchery, T., Germain, Y., Jorry, S.J., Ménot, G., Monin, L., Ponzevera, E., Rouget, M.L., Tachikawa, K., Barrat, J.A., 2015. Rare earth elements and neodymium isotopes in world river sediments revisited. Geochim. Cosmochim. Acta 170, 17–38.

Beaudouin, C., Jouet, G., Suc, J.P., Berné, S., Escarguel, G., 2007. Vegetation dynamics in southern France during the last 30 ky BP in the light of marine palynology. Quat. Sci. Rev. 26, 1037–1054.

Bonneau, L., Jorry, S.J., Toucanne, S., Silva Jacinto, R., Emmanuel, L., 2014. Millennial-scale response of a Western Mediterranean river to late quaternary climate changes: a view from the deep sea. J. Geol. 122, 687–703.

Bonneau, L., Toucanne, S., Bayon, G., Jorry, S.J., Emmanuel, L., Silva Jacinto, R., 2017. Glacial erosion dynamics in a small mountainous watershed (Southern French Alps): a source-to-sink approach. Earth Planet. Sci. Lett. 458, 366–379.

Bosia, C., Chabaux, F., Pelt, E., Cogez, A., Stille, P., Deloule, E., France-Lanord, C., 2018. U-series disequilibria in minerals from Gandak River sediments (Himalaya). Chem. Geol. 477, 22–34.

Bourdon, B., Bureau, S., Andersen, M.B., Pili, E., Hubert, A., 2009. Weathering rates from top to bottom in a carbonate environment. Chem. Geol. 258, 275–287.

Castelltort, S., Van Den Driessche, J., 2003. How plausible are high-frequency sediment supply-driven cycles in the stratigraphic record? Sediment. Geol. 157, 3–13.

Chabaux, F., Bourdon, B., Riotte, J., 2008. U-Series Geochemistry in Weathering Profiles, River Waters and Lakes, Radioactivity in the Environment. Elsevier.

Cogez, A., Herman, F., Pelt, É., Reuschlé, T., Morvan, G., Darvill, C.M., Norton, K.P., Christl, M., Märki, L., Chabaux, F., 2018. U–Th and & ^{10}Be constraints on sediment recycling in proglacial settings, Lago Buenos Aires, Patagonia. Earth Surf. Dyn. 6, 121–140.

Condie, K.C., 1993. Chemical composition and evolution of the upper continental crust: contrasting results from surface samples and shales. Chem. Geol. 104, 1–37.

DePaolo, D.J., Maher, K., Christensen, J.N., McManus, J., 2006. Sediment transport time measured with U-series isotopes: results from ODP North Atlantic drift site 984. Earth Planet. Sci. Lett. 248, 394–410.

Dequincey, O., Chabaux, F., Clauer, N., Sigmarsson, O., Liewig, N., Leprun, J.-C., 2002. Chemical mobilizations in laterites: evidence from trace elements and ^{238}U-^{234}U-^{230}Th disequilibria. Geochim. Cosmochim. Acta 66, 1197–1210.

Dosseto, A., Bourdon, B., Gaillardet, J., Allègre, C.J., Filizola, N., 2006a. Timescale and conditions of chemical weathering under tropical climate: study of the Amazon basin with U-series. Geochim. Cosmochim. Acta 70, 71–89.

Dosseto, A., Bourdon, B., Gaillardet, J., Maurice-Bourgoin, L., Allègre, C.J., 2006b. Weathering and transport of sediments in the Bolivian Andes: time constraints from uranium-series isotopes. Earth Planet. Sci. Lett. 248, 759–771.

Dosseto, A., Bourdon, B., Turner, S.P., 2008. Uranium-series isotopes in river materials: insights into the timescales of erosion and sediment transport. Earth Planet. Sci. Lett. 265, 1–17.
Dosseto, A., Buss, H.L., Chabaux, F., 2014. Age and weathering rate of sediments in small catchments: the role of hillslope erosion. Geochim. Cosmochim. Acta 132, 238–258.
Dosseto, A., Hesse, P., Maher, K., Fryirs, K., Turner, S.P., 2010. Climatic and vegetation control on sediment dynamics. Geology 38, 395–398.
Dosseto, A., Schaller, M., 2016. The erosion response to Quaternary climate change quantified using uranium isotopes and in situ-produced cosmogenic nuclides. Earth-Sci. Rev. 155, 60–81.
Dubar, M., Anthony, E.J., 1995. Holocene environmental change and river-mouth sedimentation in the Baie des Anges, French Riviera. Quat. Res. 43, 329–343.
Fleischer, R.L., 1980. Isotopic disequilibrium of uranium: Alpha-recoil damage and preferential solution effects. Science 207, 979–981.
Fleischer, R.L., 1982. Nature of alpha-recoil damage: evidence from preferential solution effects. Nucl. Tracks Radiat. Meas. 1982 (6), 35–42.
Francke, A., Carney, S., Wilcox, P., Dosseto, A., 2018. Sample preparation for determination of comminution ages in lacustrine and marine sediments. Chem. Geol. 479, 123–135.
Francke, A., Dosseto, A., Panagiotopoulos, K., Leicher, N., Lacey, J.H., Kyrikou, S., Wagner, B., Zanchetta, G., Kouli, K.L., Leng, M.J., 2019. Sediment residence time reveals Holocene shift from climatic to vegetation control on catchment erosion in the Balkans. Glob. Planet. Change 177, 186–200.
Goldstein, S.J., Jacobsen, S.B., 1987. The Nd ans Sr isotopic systematics of river-water dissolved material: implications for the sources of Nd and Sr in seawater. Chem. Geol. 66.
Granet, M., Chabaux, F., Stille, P., Dosseto, A., France-Lanord, C., Blaes, E., 2010. U-series disequilibria in suspended river sediments and implication for sediment transfer time in alluvial plains: the case of the Himalayan rivers. Geochim. Cosmochim. Acta 74, 2851–2865.
Handley, H.K., Turner, S., Dosseto, A., Haberlah, D., Afonso, J.C., Schaefer, B., 2013. Considerations for the determination of sediment residence times using the uranium-isotope comminution method: insights from palaeochannel deposits and bedrock of South Australia. Chem. Geol. 340, 40–48.
Heimsath, A.M., DiBiase, R.A., Whipple, K.X., 2012. Soil production limits and the transition to bedrock-dominated landscapes. Nat. Geosci. 5, 210–214.
Hengl, T., Mendes de Jesus, J., Heuvelink, G.B.M., Ruiperez González, M., Kilibarda, M., Blagotić, A., Shangguan, W., Wright, M.N., Geng, X., Bauer-Marschallinger, B., Guevara, M., Vargas, R., MacMillan, R.A., Batjes, N.H., Leenaars, J.G.B., Ribeiro, E.D.C., Wheeler, I., Mantel, S., Kempen, B., 2017. SoilGrids250m: global gridded soil information based on machine learning. PLoS ONE 12.
Jerolmack, D.J., Paola, C., 2010. Shredding of environmental signals by sediment transport. Geophys. Res. Lett. 37, L19401.
Jorry, S.J., Jégou, I., Emmanuel, L., Jacinto, R.S., Savoye, B., 2011. Turbiditic levee deposition in response to climate changes: the Var Sedimentary Ridge (Ligurian Sea). Mar. Geol. 279, 148–161.
Julian, M., 1977. Une carte geomorphologique des Alpes Maritimes franco-italiennes au 1/200 000e en couleurs. Presentation succincte. Mediterranee 28 (1), 45–53.
Kerckhove, C., Barfety, J.C., 1980. Gap, Carte geologique de la France à 1/250000.
Kigoshi, K., 1971. Alpha-recoil thorium-234: dissolution into water and the uranium-234/uranium-238 disequilibrium in nature. Science 173, 47–48.
Luo, S., Ku, T.-L., Roback, R., Murrell, M., McLing, T.L., 2000. In-situ radionuclide transport and preferential groundwater flows at INEEL (Idaho): decay-series disequilibrium studies. Geochim. Cosmochim. Acta 64, 867–881.
Lupker, M., France-Lanord, C., Galy, V., Lavé, J., Gaillardet, J., Gajurel, A.P., Guilmette, C., Rahman, M., Singh, S.K., Sinha, R., 2012. Predominant floodplain over mountain weathering of Himalayan sediments (Ganga basin). Geochim. Cosmochim. Acta 84, 410–432.
Maher, K., DePaolo, D.J., Christensen, J.N., 2006. U-Sr isotopic speedometer: fluid flow and chemical weathering rates in aquifers. Geochim. Cosmochim. Acta 70, 4417–4435.
Mariotti, A., 2020. Impact du dernier cycle glaciaire interglaciaire sur la dénudation dans les Alpes Maritimes Françaises.
Mariotti, A., Blard, P.H., Charreau, J., Petit, C., Molliex, S., 2019. Denudation Systematics Inferred from in Situ Cosmogenic 10Be Concentrations in Fine (5P 100 1/4m) and Medium (10P 250 1/4m) Sediments of the Var River Basin, Southern French Alps.
Mathieu, D., Bernat, M., Nahon, D., 1995. Short-lived U and Th isotope distribution in a tropical laterite derived from granite (Pitinga river basin, Amazonia, Brazil): application to assessment of weathering rate. Earth Planet. Sci. Lett. 136, 703–714.
McLennan, S.M., 2001. Relationships between the trace element composition of sedimentary rocks and upper continental crust. Geochem. Geophys. Geosyst. 2.
Milliman, J.D., Meade, R.H., 1983. World-wide delivery of river sediments to the oceans. J. Geol. 1, 1–21.
Mulder, T., Savoye, B., Piper, D.J.W., Syvitski, J.P.M., 1998. The Var Submarine Sedimentary System: Understanding Holocene Sediment Delivery Processes and Their Importance to the Geological Record. Special Publications, vol. 129. Geological Society, London, pp. 145–166.
Mulder, T., Savoye, B., Syvitski, J.P.M., 1997. Numerical modelling of a mid-sized gravity flow: the 1979 Nice turbidity current (dynamics, processes, sediment budget and seafloor impact). Sedimentology 44.
Payrastre, O., Nicolle, P., Bonnifait, L., Brigode, P., Astagneau, P., Baise, A., Belleville, A., Bouamara, N., Bourgin, F., Breil, P., Brunet, P., Cerbelaud, A., Courapied, F., Devreux, L., Dreyfus, R., Gaume, E., Nomis, S., Poggio, J., Pons, F., Rabab, Y., Sevrez, D., 2022. The 2 October 2020 Alex Storm in South-Eastern France: a Contribution of the Scientific Community to the Flood Peak Discharges Estimation. LHB, p. 2082891.
Plater, A.J., Dugdale, R.E., Ivanovich, M., 1988. The application of uranium series disequilibrium concepts to sediment yield determination. Earth Surf. Process. Landf. 13, 171–182.
Plater, A.J., Ivanovich, M., Dugdale, R.E., 1992. Uranium series disequilibrium in river sediments and waters: the significance of anomalous activity ratios. Appl. Geochem. 7.
Richter, S., Goldberg, S.A., 2003. Improved techniques for high accuracy isotope ratio measurements of nuclear materials using thermal ionization mass spectrometry. Int. J. Mass Spectrom. 229, 181–197.
Romans, B., Castelltort, S., Covault, J.A., Fildani, A., Walsh, J.P., 2016. Environmental signal propagation in sedimentary systems across timescales. Earth-Sci. Rev. 153, 7–29.
Rothacker, L., Dosseto, A., Francke, A., Chivas, A.R., Vigier, N., Kotarba-Morley, A.M., Menozzi, D., 2018. Impact of climate change and human activity on soil landscapes over the past 12,300 years. Sci. Rep. 8, 247.
Rouire, J., 1979. Nice, Carte géologique de la France à 1/250000.
Sage, L., 1976. La sédimentation à l'embouchure d'un fleuve côtier Méditerranéen: le Var. Université de Nice. Q18.
Schaller, M., Ehlers, T.A., 2006. Limits to quantifying climate driven changes in denudation rates with cosmogenic radionuclides. Earth Planet. Sci. Lett. 248, 153–167.
Shangguan, W., Hengl, T., Mendes de Jesus, J., Yuan, H., Dai, Y., 2017. Mapping the global depth to bedrock for land surface modeling. J. Adv. Model. Earth Syst. 9, 65–88.
Simpson, G., Castelltort, S., 2012. Model shows that rivers transmit high-frequency climate cycles to the sedimentary record. Geology 40, 1131–1134.
Sims, K.W.W., Gill, J.B., Dosseto, A., Hoffmann, D.L., Lundstrom, C.C., Williams, R.W., Ball, L., Tollstrup, D., Turner, S., Prytulak, J., Glessner, J.J.G., Standish, J.J., Elliott, T., 2008. An inter-laboratory assessment of the Thorium isotopic composition of synthetic and rock reference materials. Geostand. Geoanal. Res. 32, 65–91.
Sing, K.S.W., 1985. Reporting physisorption data for gas/solid systems with special reference to the determination of surface area and porosity (Recommendations 1984). Pure Appl. Chem. 57, 603–619.
Stallard, R.F., 1985. River Chemistry, Geology, Geomorphology, and Soils in the Amazon and Orinoco Basins.
Stallard, R.F., Edmond, J.M., 1983. Geochemistry of the Amazon, 2. The influence of geology and weathering environment on the dissolved load. J. Geophys. Res. 88, 9671–9688.
Suresh, P.O., Dosseto, A., Hesse, P.P., Handley, H.K., 2014. Very long hillslope transport timescales determined from uranium-series isotopes in river sediments from a large, tectonically stable catchment. Geochim. Cosmochim. Acta 142, 442–457.
Thollon, M., Bayon, G., Toucanne, S., Trinquier, A., Germain, Y., Dosseto, A., 2020. The distribution of (234U/238U) activity ratios in river sediments. Geochim. Cosmochim. Acta 290, 216–234.
West, A.J., Galy, A., Bickle, M., 2005. Tectonic and climatic controls on silicate weathering. Earth Planet. Sci. Lett. 235, 211–228.
Yanites, B.J., Tucker, G.E., Anderson, R.S., 2009. Numerical and analytical models of cosmogenic radionuclide dynamics in landslide-dominated drainage basins. J. Geophys. Res. 114.
Yoo, K., Amundson, R., Heimsath, A.M., Dietrich, W.E., Brimhall, G.H., 2007. Integration of geochemical mass balance with sediment transport to calculate rates of soil chemical weathering and transport on hillslopes. J. Geophys. Res. 112.
Yoo, K., Mudd, S.M., 2008. Discrepancy between mineral residence time and soil age: implications for the interpretation of chemical weathering rates. Geology 36, 35–38.